LETTER

doi:10.1038/nature11342

Long-term decline of global atmospheric ethane concentrations and implications for methane

Isobel J. Simpson[1], Mads P. Sulbaek Andersen[1,2], Simone Meinardi[1], Lori Bruhwiler[3], Nicola J. Blake[1], Detlev Helmig[4], F. Sherwood Rowland[1] & Donald R. Blake[1]

After methane, ethane is the most abundant hydrocarbon in the remote atmosphere. It is a precursor to tropospheric ozone and it influences the atmosphere's oxidative capacity through its reaction with the hydroxyl radical, ethane's primary atmospheric sink[1–3]. Here we present the longest continuous record of global atmospheric ethane levels. We show that global ethane emission rates decreased from 14.3 to 11.3 teragrams per year, or by 21 per cent, from 1984 to 2010. We attribute this to decreasing fugitive emissions from ethane's fossil fuel source—most probably decreased venting and flaring of natural gas in oil fields—rather than a decline in its other major sources, biofuel use and biomass burning. Ethane's major emission sources are shared with methane, and recent studies have disagreed on whether reduced fossil fuel or microbial emissions have caused methane's atmospheric growth rate to slow[4,5]. Our findings suggest that reduced fugitive fossil fuel emissions account for at least 10–21 teragrams per year (30–70 per cent) of the decrease in methane's global emissions, significantly contributing to methane's slowing atmospheric growth rate since the mid-1980s.

The estimated emissions budget for ethane (C_2H_6) is approximately 13 teragrams (1 Tg = 10^{12} g) per year. Its primary sources are fossil fuels (mainly evaporative emissions from their production, transmission and processing; 8.0–9.2 Tg yr^{-1}), biomass burning (2.4–2.8 Tg yr^{-1}) and biofuel use (2.6 Tg yr^{-1}), with minor oceanic and biogenic sources and a possible geological source[3,6–8]. Ethane has a strong interhemispheric gradient because its major sources are primarily located in the Northern Hemisphere and its atmospheric lifetime (about two months) is shorter than the interhemispheric mixing time (about a year) (refs 1, 2). Ethane emissions in the Northern Hemisphere have been estimated to be about 12 Tg yr^{-1}, of which 1.7–2.0 Tg yr^{-1} are transported to the Southern Hemisphere via interhemispheric transport[1,7]. An additional 1.0 Tg yr^{-1} is released within the Southern Hemisphere, primarily from biomass burning[7].

Whereas early measurements of atmospheric ethane in Switzerland (1951–1988) recorded an average increase of 0.8 ± 0.3% yr^{-1}, subsequent field studies (1977–2000) have reported either steady or declining ethane levels in both hemispheres (Supplementary Table 1). The present work covers latitudes from 71° N (Barrow, Alaska) to 47° S (Slope Point, New Zealand) and represents the world's longest-running global atmospheric ethane monitoring program. The measurements began in 1984 as part of our established network to monitor global concentrations of trace gases including methane, chlorofluorocarbons and other light hydrocarbons[2,9,10]. Each season between 60–80 air samples were collected at 40–45 remote surface locations in the Pacific Basin (Fig. 1). These samples were analysed at our UCI laboratory using gas chromatography and were used to calculate a globally averaged ethane mixing ratio (see Methods Summary). Based on an intercomparison with ethane data from 2006–2010 from the NOAA/INSTAAR global non-methane hydrocarbon monitoring programme, which is not limited to the Pacific basin, we estimate that our data realistically approximate the average global tropospheric ethane concentration to within 15–20%, which is within the combined uncertainty margin of both records (Supplementary Figs 1–2).

Consistent with its source distribution, ethane mixing ratios are greatest at latitudes north of 30° N, then drop precipitously from 30° N to the Intertropical Convergence Zone (Fig. 2a). Ethane is fairly well-mixed south of the Intertropical Convergence Zone, with typical variability of less than 30% among the latitudinal bands shown in

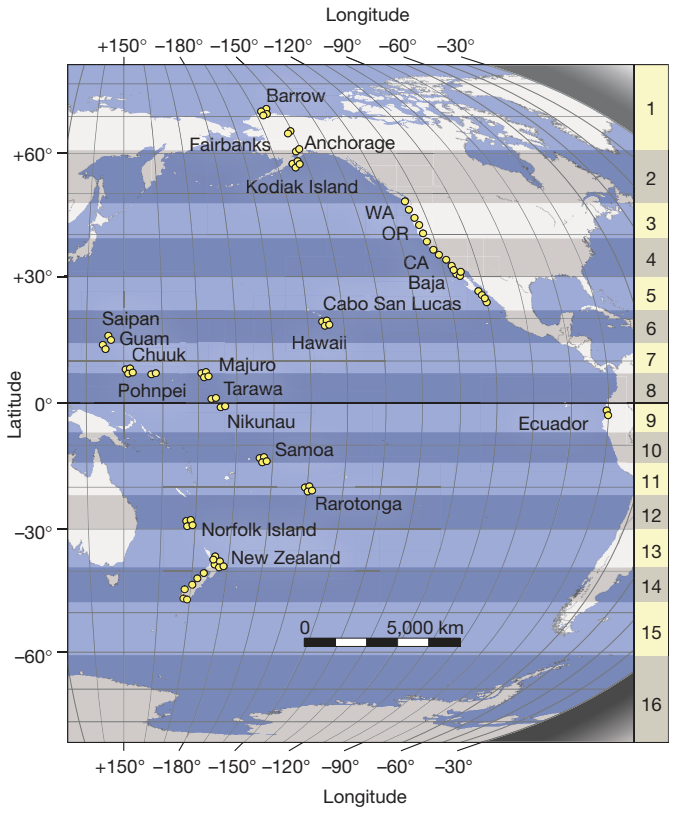

Figure 1 | Individual air sampling locations for the UCI global trace gas monitoring network. Each air sample is collected for one minute into a conditioned, evacuated two-litre stainless steel canister, typically at a site (yellow circles) on the coast when the wind is blowing from the ocean. Air samples are usually collected over a 3-week period each season (March, June, September and December), though samples were collected less frequently in 1991 and 1992 (April, August and December) because of political events at the time. We have also collected biweekly air samples on Norfolk Island (29° S) since June 2001. Boundaries that separate the Earth's surface into 16 latitudinal bands, each with an equal volume of air, are shown on the right (see Supplementary Information). The global representativeness of our Pacific-based measurements, both spatial and temporal, is discussed in the Supplementary Information. WA, Washington; OR, Oregon; CA, California.

[1]Department of Chemistry, University of California—Irvine (UCI), Irvine, California 92697, USA. [2]Jet Propulsion Laboratory, California Institute of Technology, Pasadena, California 91109, USA. [3]NOAA Earth System Research Laboratory (ESRL), 325 Broadway, Boulder, Colorado 80305, USA. [4]Institute of Arctic and Alpine Research (INSTAAR), University of Colorado, Boulder, Colorado 80309, USA.

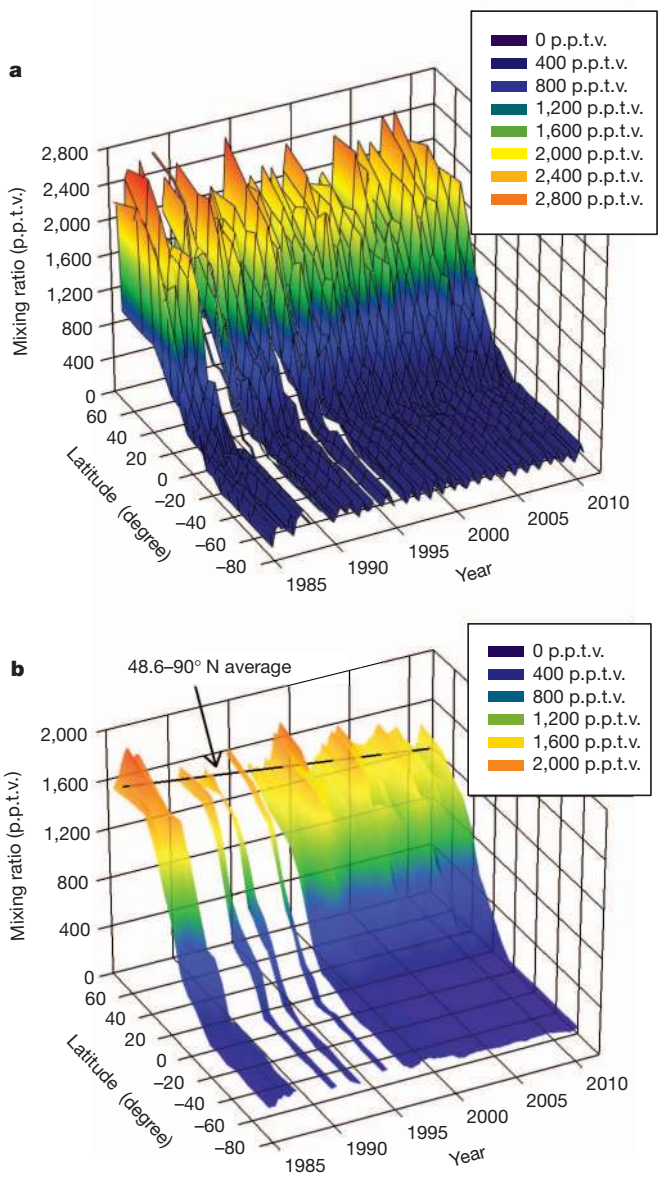

Figure 2 | Latitudinal distribution of ethane mixing ratios from 1984–2010. **a**, Seasonal averages for each of the 16 latitudinal bands shown in Fig. 1; and **b**, running annual averages for each latitudinal band. Our 26-year data set, from September 1984 to December 2010, is missing six seasons of ethane data from earlier in our programme (December 1987, June–September 1988, June 1989, September 1993 and June 1995).

Fig. 1. From 1984–2010 the average ethane mixing ratio was 1,443 ± 49 parts per trillion by volume (p.p.t.v.) in the high Northern Hemisphere (defined here as 30° N–90° N), and 269 ± 2 p.p.t.v. for the mid-Southern Hemisphere (defined as 15° S–49° S) (see Supplementary Information for uncertainty calculations). Full hemispheric averages over this period were 1,049 ± 99 p.p.t.v. for the Northern Hemisphere and 277 ± 34 p.p.t.v. for the Southern Hemisphere, with an average (±1σ) interhemispheric ratio of 4.1 ± 0.4 (see Supplementary Information).

In addition to pronounced latitudinal variations, atmospheric ethane concentrations vary both seasonally and interannually. Ethane shows a late winter maximum and summer minimum in each hemisphere, with a crossover point near the Equator (Fig. 2a). Ethane's fossil fuel source is not believed to have a strong seasonal cycle[3], so the clear, anticorrelated seasonal signals in each hemisphere are principally attributed to enhanced summertime photochemical sinks. From 1984 to 2010 the average (±1σ) amplitude of ethane's seasonal signal was much larger in the high Northern Hemisphere (800 ± 59 p.p.t.v.) than in the mid-Southern Hemisphere (35 ± 11 p.p.t.v.), which is again consistent with ethane's source distribution. The northern seasonal signal also shows significant interannual variability, with several large positive short-term anomalies of up to 30% that typically occur every 3–5 years (Fig. 2a) and have been linked to fluctuations in biomass burning emissions[10].

Atmospheric ethane mixing ratios have declined significantly since 1984, with the strongest decrease at high northern latitudes (Fig. 2b). From a linear fit to running annual averages from 1984 to 2010, we conclude that ethane declined by an average of –12.4 ± 1.3 p.p.t.v. yr^{-1} in the high Northern Hemisphere, –8.0 ± 1.0 p.p.t.v. yr^{-1} in the tropical Northern Hemisphere, defined as 0°–30° N, and –3.0 ± 0.3 p.p.t.v. yr^{-1} in the mid-Southern Hemisphere (uncertainties are the standard error of the slope). Globally, ethane has decreased by an average of –6.8 ± 0.6 p.p.t.v. yr^{-1}, from 791 ± 19 p.p.t.v. in 1986 to 625 ± 12 p.p.t.v. in 2010, making a total decline of 165 p.p.t.v. (approximately 21%). The global decline was stronger from 1984 to 1999 (–7.2 ± 1.7 p.p.t.v. yr^{-1}) than from 2000 to 2010 (–1.9 ± 1.3 p.p.t.v. yr^{-1}). Firn air measurements suggest that the global ethane concentration peaked in the 1960s and 1970s (ref. 4), before global observational networks were established, which is consistent with results from single-site field studies (see Supplementary Information).

The translation of ethane's global mixing ratio (in units of p.p.t.v.) into the annual emission rates needed to sustain it (in units of Tg yr^{-1}) requires knowledge of the spatial distribution and atmospheric removal rates of ethane. For example, using a comprehensive suite of ground-based and aircraft measurements, ref. 1 converted a global ethane burden of 860 p.p.t.v. to an emission rate of 15.5 Tg yr^{-1}. These 'top-down' global ethane emission estimates lie in the range 10.4–17.6 Tg yr^{-1} (ref. 7 and references therein), and agree with recent 'bottom-up' (inventory-based) estimates of 12.5–13.0 Tg yr^{-1} (refs 3,7). Using the top-down method as ref. 1, we calculate that ethane's annual global emission was 14.3 ± 0.3 Tg yr^{-1} in 1986, declining to 11.3 ± 0.2 Tg yr^{-1} in 2010, for an overall decrease of 3.0 ± 0.4 Tg yr^{-1}. The good agreement between our top-down emission rates and the recent bottom-up estimates suggests that the ethane budget is well balanced. Therefore, major additional sources are unlikely, making it improbable that ethane has a large geological source. However, confirmation of this would require detailed analysis of the ethane budget, which is beyond the scope of this work.

To investigate the dominant processes that control the abundance of ethane in each hemisphere, simulations were run using the TM5 atmospheric tracer transport model (see Methods Summary) together with ethane data collected from 2000 to 2010 at selected sites, namely Barrow (71° N), Majuro (7° N) and Norfolk Island (29° S). The model reproduced the observational data well at Barrow and Norfolk Island (Fig. 3). Poorer agreement was found in Majuro, probably because it lies near the transitional zone between the two hemispheres (Supplementary Fig. 3). Anthropogenic sources (that is, fossil fuel sources) were the main driver of the ethane signal in Barrow, with a smaller biomass burning component that peaks during summer (Fig. 3a). The observations and model both showed maximum concentrations in air arriving at Norfolk Island during September and October (Fig. 3b), consistent with a predominant biomass burning signal in the Southern Hemisphere[11].

The model simulations discussed above inform our investigation of the causes of ethane's decline over the past 25 years. It is unlikely that changes in global levels of the hydroxyl radical (OH) were responsible for ethane's long-term global decline, because global OH levels have shown little interannual variability since the late 1990s and are generally well buffered against changes on interannual timescales[12]. Instead, because anthropogenic emissions dominate the ethane budget in the high Northern Hemisphere, where the strongest ethane decline has occurred, we attribute ethane's decline primarily to reduced emissions from the fossil fuel sector, specifically fugitive emissions of

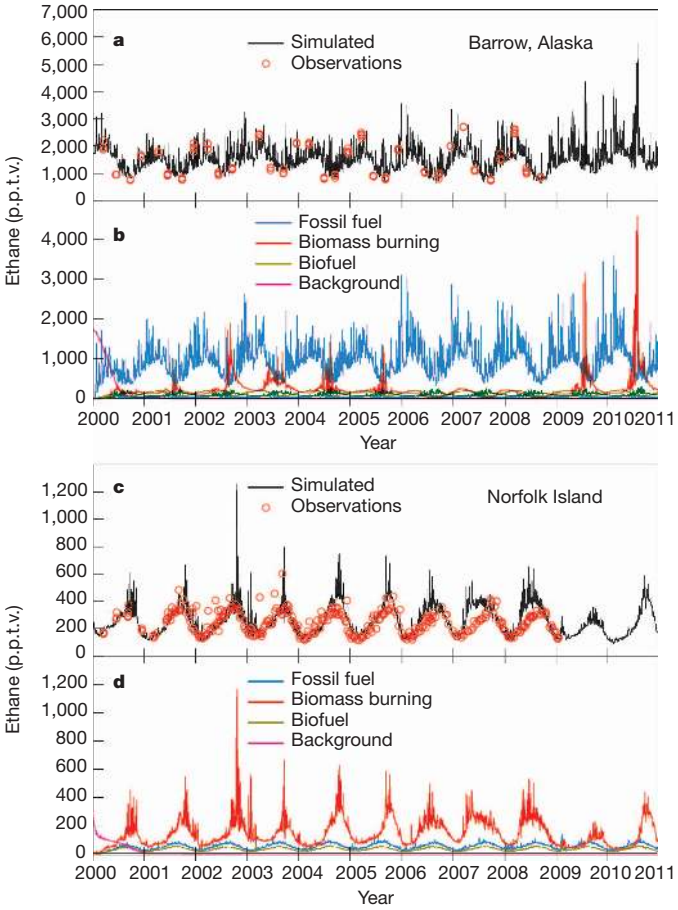

Figure 3 | Simulated and observed ethane mixing ratios from 2000 to 2010. **a**, **b**, Barrow, Alaska (71° N, 157° W). **c**, **d**, Norfolk Island (29° S, 168° E). The Barrow observations were made seasonally, and the Norfolk Island observations were made seasonally until June 2001 and bi-weekly thereafter. Even though the TM5 model is capable of much higher spatial resolution (that is, $1° \times 1°$), for this work the model used nested grids at a lower resolution ($6° \times 4°$) that is more appropriate to our observational network, which represents well-mixed background air. Ethane simulations (summed sources) are shown as a black line, ethane observations as red circles, fossil fuel simulations as a blue line, biomass burning simulations as a red line, biofuel simulations as a green line, and background simulations as a pink line.

natural gas, which is ethane's main fossil fuel source. Fugitive emissions include venting and flaring, evaporative losses, and equipment leaks and failures, but exclude the combustion of fuels. Natural gas associated with oil fields, also known as associated gas, is commonly vented or flared when it cannot be used directly or transported away[13,14]. Although no reliable global data are available, most natural gas venting occurs at upstream production facilities[14]. Flaring is estimated to have peaked in the 1970s, after which high energy prices encouraged the use of more natural gas as a fuel[15], and global gas flaring has remained fairly constant since the mid-1990s (ref. 13). Although increased use of catalytic converters on internal combustion engines has effectively reduced the emissions of many hydrocarbons, it does not appear to have similarly affected ethane levels (see Supplementary Information).

Quantifying and understanding ethane's long-term global decline provides valuable constraints on how we understand the long-term slowdown in the global growth rate of atmospheric methane[10,16], an important greenhouse gas and tropospheric ozone (O_3) precursor. Following strong growth of 1.0–1.2% yr^{-1} in the early and mid-1980s, the methane growth rate slowed to $0.40 \pm 0.31\%\ yr^{-1}$ in the 1990s and to $0.11 \pm 0.15\%\ yr^{-1}$ in the 2000s, with strong interannual variability[10]. Because methane has a relatively long atmospheric lifetime (about nine years), its atmospheric concentrations respond more slowly to changes in emissions than is the case for ethane. Consequently, methane's atmospheric growth rate is a more sensitive indicator of fluctuations in methane's emissions. Although a change in methane emission rate is strongly connected to a change in growth rate, we note that the two are not equivalent.

A graph of atmospheric ethane mixing ratio versus methane growth rate reveals a remarkably strong correlation between the two gases over the past 25 years (Fig. 4) and indicates that there has been a long-term change in a source common to both compounds. The above discussion suggests that this common source is fugitive emissions from the oil and natural gas industries. Because methane and ethane are emitted from fossil fuel sources with characteristic emission ratios[7,17,18], our long-term ethane record can be used to quantitatively investigate methane's slowing growth rate. We note that this analysis does not exclude the possibility that changes in other sources have also contributed to methane's long-term growth rate decline.

Using ethane measurements in firn air, ref. 4 estimated a 5–6 Tg yr^{-1} decline in global fossil fuel ethane emissions from 1980 to 2000. Combining this with mass-based methane-to-ethane emission ratios (MERs) of 3–5, these authors calculated a corresponding 15–30 Tg yr^{-1} drop in fossil fuel methane emissions, and concluded that the slowdown in global atmospheric methane growth was probably caused by decreasing fossil fuel emissions[4], in general agreement with a previous inversion analysis[19]. In contrast, using an independent approach based on methane isotope analysis, ref. 5 attributed the methane slowdown in the late twentieth century to decreases in Northern Hemisphere microbial sources. A new analysis of global methane isotope data from 1988 to 2005 could not confirm the conclusion of ref. 5 that northern microbial sources have declined significantly in recent decades[20]. However, this new study also implies that fossil fuel emissions of methane may have remained mostly constant[20]. These multiple conflicting results are unexpected, and we use the global ethane data presented above to address these unresolved scientific questions.

First, because the measurements of ref. 4 were from polar latitudes only, it was not possible for them to rule out whether a large shift in fossil fuel emissions, towards lower latitudes in the Northern Hemisphere, contributed to their observed long-term ethane decline.

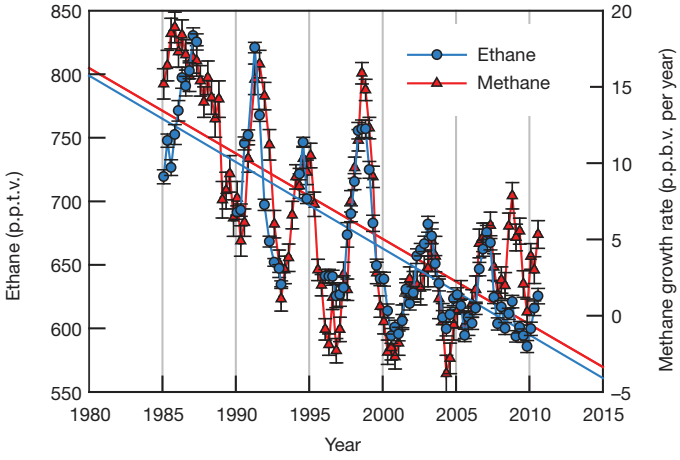

Figure 4 | Running global averages of ethane mixing ratios and methane growth rate. The methane measurements, which were co-sampled with ethane, are also from the UCI global monitoring network and are described in ref. 10. Solid lines are linear fits to the ethane (blue circles) and methane (red triangles) data using a least-squares regression. Each global average is based on 55–75 individual mixing ratios. The averaging procedure and uncertainty calculations are described in the Supplementary Information.

Our global data suggests that this was not the case. Although the decline in ethane emissions has been greatest at high northern latitudes ($1.4 \pm 0.2\ Tg\ yr^{-1}$ for the high Northern Hemisphere), a similar trend has occurred at all latitudes within the Northern Hemisphere ($0.9 \pm 0.1\ Tg\ yr^{-1}$ for the tropical Northern Hemisphere) and there is no evidence to suggest that ethane emissions have shifted to lower latitudes in the Northern Hemisphere. This supports the extrapolation by ref. 4 of polar firn air measurements to global trends.

Second, if we attribute our calculated $3.0 \pm 0.4\ Tg\ yr^{-1}$ decline in global ethane emissions from 1984 to 2010 solely to a decline in ethane's fossil fuel source, we can estimate the concurrent decline in methane emissions from fossil fuel. However, this approach assumes that ethane's other two major sources—biomass burning and biofuel use—have remained constant during the past three decades. In fact, global emissions of ethane from biomass burning (wildland fires) are estimated to have increased by $0.52\ Tg\ yr^{-1}$ from the 1980s to the 1990s (ref. 21), and then to have stayed fairly constant from 1997–2010 (refs 22,23) with the exception of anomalously large biomass burning years such as 1997–1998 (refs 10,22). Therefore we estimate that ethane emissions from biomass burning have increased by approximately $0.26\ Tg\ yr^{-1}$ since 1985. Global biofuel use also increased by 14% from 1985 to 2000 (ref. 24), which corresponds to a $0.36\ Tg\ yr^{-1}$ increase in ethane's biofuel source, assuming that biofuel emissions of ethane increase in parallel with global biofuel use. If we extrapolate the upward trend in global biofuel use to include 2000–2010, biofuel emissions of ethane increase another 9% ($0.23\ Tg\ yr^{-1}$) for a combined increase of $0.59\ Tg\ yr^{-1}$ from 1985 to 2010.

In total, we estimate that ethane emissions from biomass burning and biofuel have increased by approximately $0.85\ Tg\ yr^{-1}$ since 1985. Although the uncertainty associated with the estimated biomass and biofuel increases is unclear, and the uncertainty in our calculations increases as we transition from our global measurements to emission rate changes, applying this offset to our estimate of $3.0 \pm 0.4\ Tg\ yr^{-1}$ suggests a likely range of $3.4–4.2\ Tg\ yr^{-1}$ for the decline in the fossil fuel component of ethane emissions since the mid-1980s.

Applying the same range of MER values as ref. 4 (that is, 3–5), we calculate that global fossil fuel emissions of methane declined by 10–$21\ Tg\ yr^{-1}$ from 1984 to 2010. However, the MERs employed by ref. 4 were based on emission ratios measured near oil storage and processing facilities, and they lie at the lower end of MER values representing the fossil fuel industry as a whole[17,18,25]. For example, the MER of natural gas varies considerably depending on the type of deposit, with mass-based values of the order of 3 for gas associated with oil fields, 6 for gas condensate (or 'wet' gas), and 10 or more for 'dry' gas fields, although there is substantial overlap among the categories[17,18]. Further, the MER for coalbed gas can exceed 5,000 in certain basins[25]. Because the MER of associated gas (that is, approximately 3) is on the lower end of the mass-based MER scale, our above estimate of 10–$21\ Tg\ yr^{-1}$ should be a fairly accurate assessment of the component of methane's decline associated with fossil fuel use. However, if more methane-enriched fossil fuel sources also contributed to the decline in methane emissions, then 10–$21\ Tg\ yr^{-1}$ may be an underestimate.

Our estimates of global ethane concentrations and emissions indicate a significant decrease in fugitive fossil fuel methane emissions of at least 10–$21\ Tg\ yr^{-1}$, or more than 30%–70% of the total decline in global methane emissions from 1984–2010 (approximately $30\ Tg\ yr^{-1}$; ref. 5). That is, our results are incompatible with a roughly constant fossil fuel source of methane since the 1980s, as put forward in a recent scenario[20]. Further, we have demonstrated the utility of long-term co-measurement of ethane and methane, and we encourage close scrutiny of ethane levels and corresponding methane growth rates in the future. For example, signals such as a significant upturn in methane growth, without a corresponding increase in global ethane levels, may indicate releases of methane from methane-rich sources such as wetlands or melting permafrost.

METHODS SUMMARY

Air sampling and analysis. Ethane measurements were made using our established technique of whole-air sampling followed by analysis using gas chromatography with flame ionization detection[2,9,10]. The samples were analysed at our UCI laboratory within one month of collection. Rigorous tests have shown that light alkanes are stable in the canisters over this period. The measurements for each trace gas use an internally consistent, internationally recognized calibration scale and detailed quality control procedures. The precision of the ethane measurements is 1%, the accuracy 5%, and the detection limit 3 p.p.t.v. Ethane mixing ratios that appear contaminated by local sources are removed from the data set (typically 2–6 per season), and the remaining data are used to construct a seasonal global ethane average using an equal surface area weighting method (see Supplementary Information). Running annual global averages are in turn calculated from these seasonal means. The measurements are archived at http://cdiac.ornl.gov/tracegases.html.

Atmospheric modelling. Ethane simulations were run using the TM5 model of atmospheric tracer transport[26]. Assimilated meteorology data from the European Centre for Medium Range Weather Forecasting were used to calculate the atmospheric transport. A repeating seasonal cycle of OH (ref. 27) and the Jet Propulsion Laboratory kinetics data evaluation for the photochemical destruction of ethane (ref. 28) were used to calculate the reaction rate between ethane and OH. Anthropogenic ethane sources were estimated using the Emission Database for Global Atmospheric Research data set for methane, release version 4.0 (http://edgar.jrc.ec.europa.eu, 2009) together with the appropriate methane-to-ethane emission ratios[7]. Ethane emissions from biomass burning were estimated from the Global Fire Emissions Database version 2 and published emission ratios[29]. Biofuel emissions were retrieved from ref. 30. The relatively small ethane emissions from biogenic sources and the ocean were not included because of concern about their uncertainty.

Received 2 February; accepted 19 June 2012.

1. Rudolph, J. The tropospheric distribution and budget of ethane. *J. Geophys. Res.* **100** (D6), 11369–11381 (1995).
2. Gupta, M. L., Cicerone, R. J., Blake, D. R., Rowland, F. S. & Isaksen, I. S. A. Global atmospheric distributions and source strengths of light hydrocarbons and tetrachloroethene. *J. Geophys. Res.* **103** (D28), 28219–28235 (1998).
3. Pozzer, A. *et al.* Observed and simulated global distribution and budget of atmospheric C_2-C_5 alkanes. *Atmos. Chem. Phys.* **10,** 4403–4422 (2010).
4. Aydin, M. *et al.* Recent decreases in fossil-fuel emissions of ethane and methane derived from firn air. *Nature* **476,** 198–201 (2011).
5. Kai, F. M., Tyler, S. C., Randerson, J. T. & Blake, D. R. Reduced methane growth rate explained by decreased Northern Hemisphere microbial sources. *Nature* **476,** 194–197 (2011).
6. Stein, O. & Rudolph, J. Modeling and interpretation of stable carbon isotope ratios of ethane in global chemical transport models. *J. Geophys. Res.* **112,** D14308 (2007).
7. Xiao, Y. *et al.* Global budget of ethane and regional constraints on U.S. sources. *J. Geophys. Res.* **113,** D21306 (2008).
8. Etiope, G. & Ciccioli, P. Earth's degassing: a missing ethane and propane source. *Science* **323,** 478 (2009).
9. Blake, D. R. & Rowland, F. S. Global atmospheric concentrations and source strengths of ethane. *Nature* **321,** 231–233 (1986).
10. Simpson, I. J., Rowland, F. S., Meinardi, S. & Blake, D. R. Influence of biomass burning during recent fluctuations in the slow growth of global tropospheric methane. *Geophys. Res. Lett.* **33,** L22808 (2006).
11. Rinsland, C. P. *et al.* Multiyear infrared solar spectroscopic measurements of HCN, CO, C_2H_6, and C_2H_2 tropospheric columns above Lauder, New Zealand (45°S latitude). *J. Geophys. Res.* **107** (D14), 4185 (2002).
12. Montzka, S. A. *et al.* Small interannual variability of global atmospheric hydroxyl. *Science* **331,** 67–69 (2011).
13. Elvidge, C. D. *et al.* A fifteen year record of global natural gas flaring derived from satellite data. *Energies* **2,** 595–622 (2009).
14. Johnson, M. R. & Coderre, A. R. An analysis of flaring and venting activity in the Alberta upstream oil and gas industry. *J. Air Waste Manage. Assoc.* **61,** 190–200 (2011).
15. Stern, D. I. & Kaufmann, R. K. Estimates of global anthropogenic methane emissions 1860–1993. *Chemosphere* **33,** 159–176 (1996).
16. Dlugokencky, E. J. *et al.* Atmospheric methane levels off: temporary pause or a new steady-state? *Geophys. Res. Lett.* **30,** 1992 (2003).
17. Katzenstein, A. S., Doezema, L. A., Simpson, I. J., Blake, D. R. & Rowland, F. S. Extensive regional atmospheric hydrocarbon pollution in the southwestern United States. *Proc. Natl Acad. Sci. USA* **100,** 11975–11979 (2003).
18. Jones, V. T., Matthews, M. D. & Richers, D. M. Light hydrocarbons for petroleum and gas prospecting. In *Geochemical Remote Sensing of the Sub-Surface* Vol. 7 *Handbook of Exploration Geochemistry* (eds Govett, G. J. S. & Hale, M.) 133–211 (Elsevier, 2000).
19. Bousquet, P. *et al.* Contribution of anthropogenic and natural sources to atmospheric methane variability. *Nature* **443,** 439–443 (2006).
20. Levin, I. *et al.* No inter-hemispheric δ13CH4 trend observed. *Nature* **486,** E3–E4 (2012).

21. Schultz, M. G. *et al.* Global wildland fire emissions from 1960 to 2000. *Glob. Biogeochem. Cycles* **22,** GB2002 (2008).
22. van der Werf, G. R. *et al.* Global fire emissions and the contribution of deforestation, savanna, forest, agricultural, and peat fires (1997–2009). *Atmos. Chem. Phys.* **10,** 11707–11735 (2010).
23. Wiedinmyer, C. *et al.* The Fire INventory from NCAR (FINN): a high resolution global model to estimate the emissions from open burning. *Geosci. Model Dev.* **4,** 625–641 (2011).
24. Fernandes, S. D., Trautmann, N. M., Streets, D. G., Roden, C. A. & Bond, T. C. Global biofuel use, 1850–2000. *Glob. Biogeochem. Cycles* **21,** GB2019 (2007).
25. Strąpoć, D., Mastalerz, M., Eble, C. & Schimmelmann, A. Characterization of the origin of coalbed gases in southeastern Illinois Basin by compound-specific carbon and hydrogen stable isotope ratios. *Org. Geochem.* **38,** 267–287 (2007).
26. Krol, M. C. *et al.* The two-way nested global chemistry-transport zoom model TM5: algorithm and applications. *Atmos. Chem. Phys.* **5,** 417–432 (2005).
27. Spivakovsky, C. M. *et al.* Three dimensional climatological distribution of tropospheric OH: update and evaluation. *J. Geophys. Res.* **105** (D7), 8931–8980 (2000).
28. Sander, S. P. *et al.* Chemical kinetics and photochemical data for use in atmospheric studies. Evaluation No. 17, JPL Publication No. 10–6, http://jpldataeval.jpl.nasa.gov (Jet Propulsion Laboratory, 2011).
29. Andreae, M. O. & Merlet, P. Emission of trace gases and aerosols from biomass burning. *Glob. Biogeochem. Cycles* **15,** 955–966 (2001).
30. Yevich, R. & Logan, J. A. An assessment of biofuel use and burning of agricultural waste in the developing world. *Glob. Biogeochem. Cycles* **17,** 1095 (2003).

Supplementary Information is linked to the online version of the paper at www.nature.com/nature.

Acknowledgements This research was funded by NASA (grant NAG5-8935), with contributions from the Gary Comer Abrupt Climate Change Fellowship. We acknowledge discussions with many colleagues, especially M. Aydin and C. Wiedinmyer. We thank colleagues at the Norfolk Island Bureau of Meteorology and the NOAA research stations in Samoa and Barrow for sample collection; the UCI team for sample collection and analysis, especially B. Chisholm, R. Day, G. Liu, B. Love and M. McEachern; and K. Masarie for work with the NOAA/INSTAAR data. M.P.S.A. is supported at JPL by an appointment to the NASA Postdoctoral Program, administered by Oak Ridge Associated Universities through a contract with NASA.

Author Contributions I.J.S. was responsible for data quality assurance, global averaging and emission calculations and manuscript preparation. M.P.S.A. prepared the figures and improved the manuscript. S.M. was responsible for sample analysis and calibration, and data quality assurance. L.B. did the ethane modelling. N.J.B. improved the manuscript. D.H. made the NOAA/INSTAAR measurements and improved the manuscript. F.S.R. was responsible for study design and data quality assurance. D.R.B. was responsible for study design and data quality assurance, and improved the manuscript.

Author Information Reprints and permissions information is available at www.nature.com/reprints. The authors declare no competing financial interests. Readers are welcome to comment on the online version of this article at www.nature.com/nature. Correspondence and requests for materials should be addressed to I.J.S. (isimpson@uci.edu).